Astron. Astrophys. 346, 7–12 (1999)

ASTRONOMY AND ASTROPHYSICS

The nature of the extreme kinematics in the extended gas of high redshift radio galaxies

M. Villar-Martín[1], **L. Binette**[2], **and R.A.E. Fosbury**[3]

[1] Institute d'Astrophysique de Paris (IAP), 98 bis Bd Arago, F-75014 Paris, France
[2] Instituto de Astronomía, UNAM, Apartado Postal 70–264, D.F. 04510, Mexico
[3] Space Telescope European Coordinating Facility, Karl-Schwarschild-Strasse 2, D-85748 Garching, Germany

Received 21 December 1998 / Accepted 5 March 1999

Abstract. We present UV rest frame spectra of 3 powerful narrow line radio galaxies and the hyperluminous type 2 active galaxy SMM J02399-0136, all at high redshift ($z>2$). We find high velocities ($\mathrm{FWHM} > 1000\,\mathrm{km\,s^{-1}}$) in the *extended* gas of *all* objects. A natural explanation is the interaction between the radio jet and the ambient gas, that drives shocks into the gas and accelerates the clouds. However, the existence of high velocities in regions where such interactions are not taking place implies that other processes can play a role. We discuss here several possible mechanisms.

Key words: galaxies: active – galaxies: ISM – galaxies: kinematics and dynamics – cosmology: observations – radio continuum: galaxies – ultraviolet: galaxies

1. Introduction

The existence of high velocities (FWHM$>1000\,\mathrm{km\,s^{-1}}$) (McCarthy et al. 1996) in the extended gas (EELR) of high redshift ($z>2$) radio galaxies (HZRG) is in contrast with the more relaxed kinematics observed in the majority of low redshift radio galaxies (FWHM$<400\,\mathrm{km\,s^{-1}}$) (Tadhunter et al. 1989). The nature of such extreme kinematic motions is not well understood. We investigate here this issue studying the kinematics of the extended gas in a small sample of 4 distant active galaxies ($z>2$): MRC1558-003, MRC2025-218 and MRC2104-242 (radio galaxies) and SMM J02399-0136 (hyperluminous type 2 active galaxy with very weak radio emission).

2. Observations and data reduction

The spectroscopic observations were carried out on the nights 1997 July 3–5 and 1998 July 25–27 using the EMMI multipurpose instrument at the NTT (New Technology Telescope) in La Silla Observatory (ESO-Chile). The detector was a Tektronix CCD with 2048×2048 pixels of size 24 μm, resulting in a spatial scale of 0.27 arcsec per pixel. We used EMMI in RILD spectroscopic mode (Red Imaging and Low Disperson Spectroscopy). We used the same grism (#3) for all objects. This has a blaze wavelength of 4600 Å, dispersion 2.3 Å/pixel and wavelength range 4000–8300 Å. The slit was aligned with the radio axis for the three radio galaxies. We positioned the slit along the two main optical components of SMM J02399-0136 (L1 and L2, adopting the nomenclature of Ivison et al. 1998 [IV98 hereafter]). A log of the spectroscopic observations is shown in Table 1.

Standard data reduction techniques were applied using IRAF software (see Villar-Martín et al. 1998 for a more detailed description).

Send offprint requests to: M. Villar-Martín (villard@iap.fr)

3. The fitting procedure

In order to study the kinematics of the gas, we fitted the emission lines with a Gaussian profile at every spatial position (pixel). Several spatial pixels were added where the emission was too faint. We used the Starlink package DIPSO for this purpose. The FWHM, flux and central wavelength were measured from the Gaussian fitted to the line profile. The FWHM was corrected in quadrature for instrumental broadening (the instrumental profiles in the observed frame are given in Table 1).

Single Gaussians did not always provide a perfect fit and underlying broad wings were sometimes present. This is probably due to the presence of several kinematic components and/or absorption of Lyα by neutral hydrogen. To eliminate uncertainties due to the second mechanism, we also present the result of the fit for the second strongest emission line CIVλ1550 not susceptible of hydrogen absorption.

At the s/n of the data, we are confined to using single Gaussian fits to the lines, a procedure which is the same as that followed by Tadhunter et al. (1989). A single Gaussian fit will a) lose any information about multiple components b) neglect any possible weak broad underlying wings (as is observed in MRC2104-242, see Fig. 1 left cloud), since the fit will be optimized for the dominant part of the line. However, the main goal of this paper does not require such a precise analysis. The broad wing on MRC2104-242 will have little influence on the fit, which will be dominated by the strong, narrower component.

Table 1. *Log of the spectroscopic observing run*. The redshift (calculated from the spatially integrated Lyα emission) is also indicated.

Object	z	Date	t_{exp} (sec)	Slit (")	Average Seeing(")	Resol.(Å) at $\lambda^{obs}_{Ly\alpha}$	PA of slit
MRC2104-242	2.492	3/Jul/97	4×1800	1.5	1.10	10.4	22
MRC2025-218	2.632	3/Jul/97	3×1800	1.5	1.15	10.9	30
MRC1558-003	2.530	25–26/Jul/98	4×1800	1.5	1.00	10.3	75
SMM J02399-0136	2.803	25–26/Jul/98	5×1800	1.5	1.20	10.3	88.6

4. Results

We present in Figs. 1 to 4 the results of our analysis for the 4 targets in the sample. The upper panel in each figure is the 2-D spectrum of the Lyα spectral region with the dispersion in λ running vertically. The middle panel presents the spatial variation of the FWHM and the bottom panel shows the spatial variation of the velocity shift of the Lyα emission (open circles) across the nebula. The 3 panels in each figure have the same spatial scale and are aligned so that vertical lines join the same spatial positions. FWHM for CIVλ1550 is also plotted for comparison (solid triangles).

- MRC2104-242 (Fig. 1): Lyα shows a bimodal distribution and is extended over $\sim$12 arcsec along the slit aligned with the radio axis. The two blobs lie in between the radio lobes (McCarthy et al. 1990). The bimodal distribution is also apparent in CIV. The two clumps present high FWHM values (1100 km s^{-1} and 900 km s^{-1} respectively, for the spatially integrated spectra) and are shifted by $\sim$500 km s^{-1} (consistent with McCarthy et al. 1990, Koekemoer et al. 1996). Kinematic substructure is observed in the two blobs. The velocity curve (Fig. 1, bottom panel) is rather flat across each blob. CIV is also extended and presents high FWHM values ($\sim$700 km s^{-1}, see Fig. 1).
- MRC2025-218 (Fig. 2): Lyα shows a bimodal distribution and is extended over $\sim$4.5 arc sec. This structure lies between the radio lobes (Pentericci et al. 1999). Continuum is detected in our spectra. Large and rather constant FWHM values are measured across the two components ($\sim$1200 km s^{-1} and 700 km s^{-1} respectively). The velocity curve is rather steep across the nebula varying smoothly over a range of $\sim$600 km s^{-1}. CIV is also extended and presents similar FWHM as Lyα.
- MRC1558-003 (Fig. 3): Lyα is extended over $\geq$15 arc sec. A bright component is detected as well as diffuse, very extended emission which show large velocity widths at $\sim$10 arc sec from the main component. The optical (Rötggering et al. 1996) and radio astrometry (Röttgering et al. 1994, Rhee et al. 1996) locate the high velocity region several arcsec *beyond* the radio structures. CIV is also extended and presents very large FWHM within the high velocity region, consistent with the Lyα measurement. There is no apparent pattern in the velocity curve of the ionized gas.
- SMM J02399-0136 (Fig. 4): This object is a hyperluminous active galaxy, gravitationally lensed by a foreground cluster (IV98). It consists of two main optical sources L1 and L2. The radio emission is very weak, below the detection tresholds of most radio surveys. The radio, submm and optical properties are consistent with a scenario where L1 contains an active nucleus and L2 is an interacting companion. The system is undergoing strong starburst activity. We detect Lyα emission across $\sim$20 arc sec. Two main components are revealed by our spectra, coincident with (L1 and L2). Lyα is relatively broad in L1 (FWHM$\sim$1800 km s^{-1}) and narrower in L2 (FWHM$\sim$300–700 km s^{-1}). A high velocity region (FWHM$\sim$1500 km $^{-1}$) is detected at the border of L2. A spectrally unresolved region lies at $\sim$12 arc sec from L1.

The four objects present complex kinematics and show that there is a large variety of kinematic behaviour in high redshift active galaxies. All objects present certain common characteristics:

- High velocities (FWHM$>$1000 km s^{-1}) in the *extended gas*
- Velocity shift of the Lyα emission across the nebula varying over a range $<$700 km s^{-1}, although the velocity curves are rather different from object to object. Similar values are observed in low redshift radio galaxies (Tadhunter et al. 1989)
- Presence of at least two different kinematic components which seem to be spatially distinct. Such components look like individual clumps in the case of MRC2025-218, MRC2104-242 and SMM J02399-0136. Diffuse and fainter line emission is present in the spectra of SMM J02399-0136 and MRC1558-003. Narrow band Lyα narrow band images show also diffuse Lyα emission in MRC2025-218 and MRC2104-242 in addition to the brightest components (McCarthy et al. 1990, Pentericci et al. 1998).

5. Discussion

High velocities have been observed in the EELR of many HZRG (McCarthy et al. 1996). The alignment between the radio and optical structures (McCarthy et al. 1987, Chambers et al. 1987) and the anticorrelation between the size of the radio source and the velocity dispersion found for HZRG (van Ojik 1995) suggest that the jet is interacting with the ambient gas. Studies of radio galaxies at intermediate redshift with clear signs of such interactions as well as hydrodynamical simulations show that this process can produce large FWHM ($>$1000 km s^{-1}) (e.g. Villar-Martín et al 1999, Clark et al. 1997). Some HZRG show clear evidence for jet-cloud interactions (e.g. van Ojik et al.

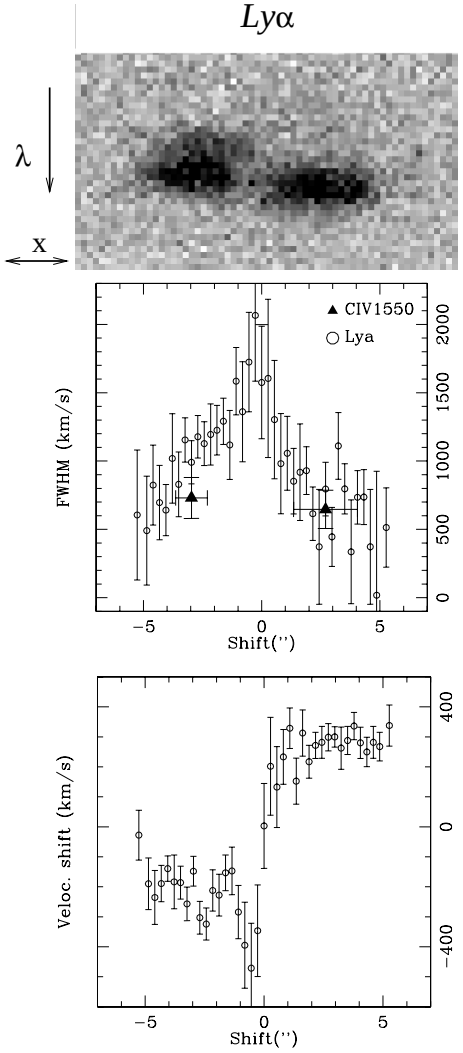

Fig. 1. *MRC2104-242. Upper panel:* 2-D spectrum of the Lyα spectral region with the dispersion in λ running vertically. Middle: Spatial variation of the FWHM. *Lower panel:* Velocity shift with respect to the emission in the center of symmetry of the Lyα distribution. The spatial shift has been calculated with respect to the same position. The horizontal lines indicate the pixels added along the spatial direction. The three panels have the same spatial scale and are aligned so that vertical lines connect the same spatial positions in the slit. The errorbars (vertical lines) include the errors of the fit, as well as the error in the measurement of the instrumental profile.

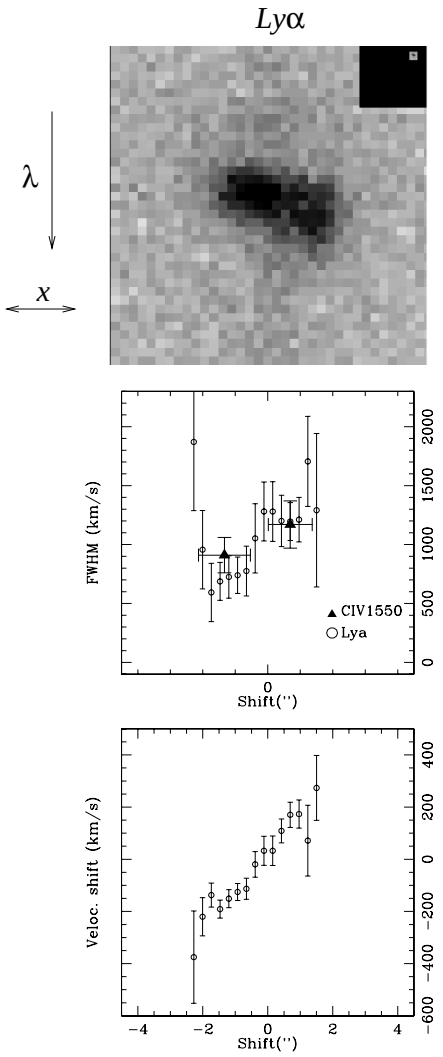

Fig. 2. *MRC2025-218.* Panels and symbols as in Fig. 1. The spatial and velocity shifts have been calculated with respect to the centroid of continuum emission.

1996) and this process is surely having an effect in some high redshift radio galaxies. It could be also the case of MRC2025-214 and MRC2104-242, which show the alignment effect (McCarthy et al. 1990) and large line widths *inside* the radio structures. However, we have also measured high velocities in the EELR of MRC1558-003 *beyond* the radio structures (Fig. 3) and the extended gas of the galaxy-galaxy interacting system SMM J02399-236. Bremer et al. (1992) reported the detection of extended Lyα emission in the radio quiet quasar 0055-264 (z =3.66) with FWHM$\sim$1000 km s^{-1}. Jet cloud interactions cannot explain the extreme kinematics in these objects. Another accelerating mechanism is at work which could also play a role in many other HZRG.

IV98 have proposed that SMM J02399-0136 is a system in which two companions are interacting: L1 (that contains an active nucleus) and L2. The interaction has induced starburst activity responsible for the submm and weak radio emissions. Another possibility is that the radio emission is due to a frustrated radio jet, since the steep radio spectrum is consistent with an AGN origin (IV98). The radio emission is extended along PA71, close to PA88.6 (L1-L2 direction) and the projected size ($\sim$7.9 arc sec) is larger than the L1-L2 extension ($\sim$4 arc sec). Therefore, the high velocity gas detected beyond L2 is probably inside the radio structures. In this case, the interaction between the radio jet and the ambient gas could be responsible for the large FWHM values measured beyond L2.

However, if SMM J02399-0136 is a system of two interaction companions with strong starburst activity [as is the case for

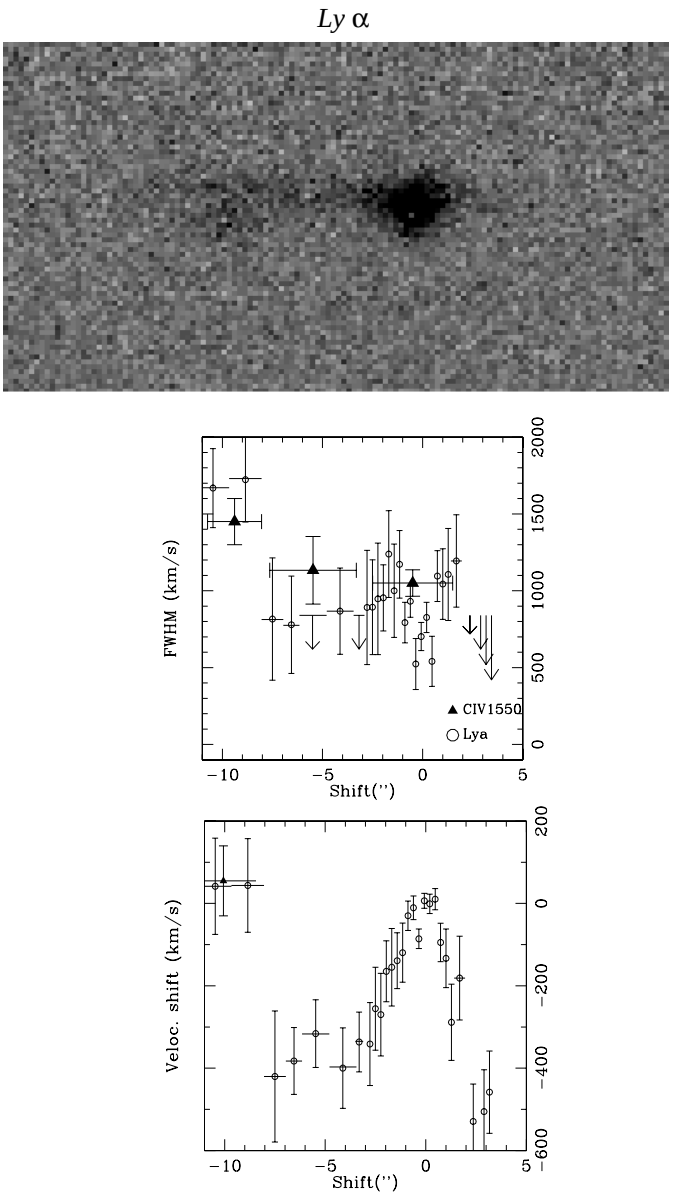

Fig. 3. *MRC1558-003.* Panels and symbols as in Fig. 1. The spatial and velocity shifts have been calculated with respect to the nuclear emission. The high velocity component 10 arc sec from the x =0 position is located beyond the radio structures.

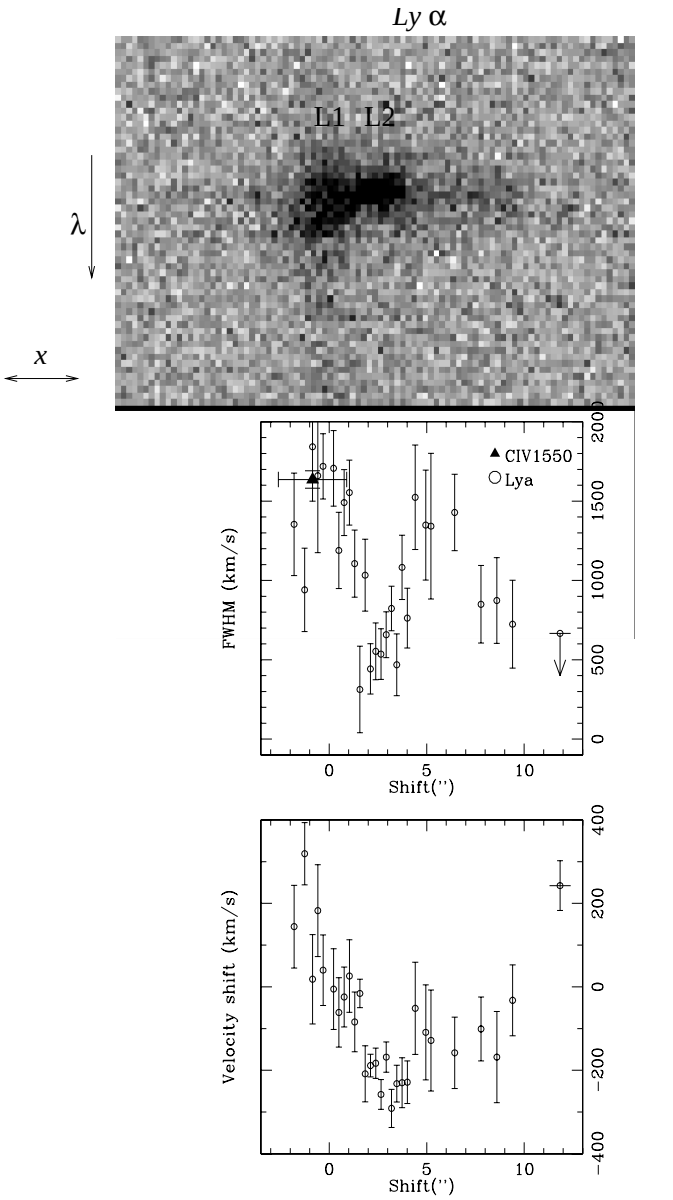

Fig. 4. *SMM J02399-0136.* Panels and symbols as in Fig. 1. The two components of the system (IV98) have been indicated (L1 and L2). The spatial and velocity shifts have been calculated with respect to the centroid of continuum emission. Note the presence of large velocities in the extended gas of this very weak radio source.

many μJy radio sources (Lowenthal 1997)], jet-cloud interactions cannot explain the gas kinematics in SMM J02399-0136.[1]

We discuss here several possible mechanisms that could explain the extreme kinematics in some HZRG.

[1] SMM J02399-0136 is gravitationally lensed by a foreground cluster. The appropriate geometry with respect to the lensing source could produce a greater distortion of component L1 due to its compact morphology. L1 emission might extend beyond L2 with the result that the high velocities measured in L1 could be contaminating measurements of the extended gas. We would then expect the same effect for NV and CIV, which are strongly nucleated and have similar fluxes in L1 than Lyα (see Fig. 3 in IV98). However, these lines are detected only in L1.

– *Broad scattered lines.*
Many distant radio galaxies (z >2) show polarized continuum with the electric vector perpendicular to the axis of the optical (UV rest frame) structures (Cimatti et al. 1998, Fosbury et al. 1998b,1999). This is consistent with an scenario in which powerful radio galaxies contain QSO nuclei whose FUV emission we see scattered by extended dust structures. The emission from the broad line region should also be scattered and therefore broad lines could be detected within the extended gas. Scattering preserves the equivalent width of BLR lines against the nuclear continuum and if this mechanism dominated, we should measure similar EW in

the extended gas. We have measured a lower limit for the EW of the CIVλ1550 line (not affected by neutral hydrogen absorption). We obtain EW(CIV)$\geq$100, which is quite large compared with typical values measured in quasars at high redshift (Corbin & Francis 1994). This suggests that the line is dominated by direct light, rather than scattered.

This mechanism is not likely to play a role in radio galaxies in general. In effect, NIR spectroscopy of distant narrow line radio galaxies (z =2.2-2.6) reveals FWHM$>$1000 km s^{-1} for both permitted and *forbidden* lines (Evans 1998). Eventhough the spectra of HZRG are customarily integrated along the spatial dimension, the extended emission frequently dominates the integrated spectra (e.g. McCarthy et al. 1996, Stockton et al. 1996) and therefore the observed large velocities could well originate from the extended regions themselves. At $z\sim$1 the [OII] emission has similarly revealed high velocities (FWHM$>$1000 km s^{-1}) within the *extended* gas regions of some radio galaxies (McCarthy et al. 1996).

– *Infall*.

Heckman et al. (1991) made a spectroscopic study of the extended gas in a sample of 5 high redshift radio-loud quasars (z $\sim$2–3) (see also Lehnert & Becker 1998). They found that the kinematical properties are very similar to the properties of the EELR of HZRG: namely velocity dispersions across the nebulae consistent with gravitational motions ($<$500 km s^{-1}) but with large FWHM$\sim$1000–1500 km s^{-1}. They propose a scenario in which gravitation is at the origin of these extreme motions: i.e. gas freely falling from a large distance into the galaxy. An infall process with such characteristics could happen during the process of galaxy formation, if the radio galaxy lies at the bottom of a deep potential well (like a dense cluster).

– *A group of Ly break galaxies around the radio galaxy.*

Recent deep HST images of radio galaxies at z $>$2 show clumpy and irregular morphologies, consisting of a bright component and a number of small components, which is suggestive of a merging system (Pentericci et al. 1998). Pentericci et al. find that those clumps have similar characteristics to Ly break galaxies and suggest that the host galaxy of the radio source had itself formed through the merging of such smaller units (see also van Breugel et al. 1999).

MRC2025-218, MRC2104-242 and SMM J02399-0136 have similar morphologies to the one described above (see optical images in Pentericci et al. 1998 and IV98). The presence of several components is also revealed by our spectra. We also detect diffuse emission between (and sometimes beyond) the main clumps which could have the same nature as the diffuse and asymmetric halos found around compact clumps in Ly break galaxies (Steidel et al. 1996).

An important difference between Ly break galaxies and the clumps in HZRG is the large velocities measured *in each clump* (FWHM$>$1000 km s^{-1}), much larger than the values observed in Ly break galaxies (FWHM$\leq$200 km s^{-1}) (e.g. Pettini et al. 1998, Prochaska & Wolfe 1997). However, spectroscopy shows that velocity shifts of $>$1000 km s^{-1} between absorbing and emitting gas are common in Ly break galaxies. This suggests the presence of large scale outflows of hundreds km s^{-1} (e.g. Pettini et al. 1998, Franx et al. 1997), which could be responsible for large FWHM values if all the gas was ionized. On the other hand no clear link has been established between the absorbing and the ionized gas and, therefore, these velocity differences might simply occur between unrelated intervening objects.

– *Bipolar outflows.*

Chambers (1998) has recently proposed that bipolar outflows can be responsible for the high velocities, morphologies and polarimetric properties of high redshift radio galaxies. The EELR of HZRG consists in this model of an expanding bipolar dust shell which scatters light from a quasar core and has an evacuated interior.

Bipolar outflows can be generated by the superwind associated with a starburst in a circumnuclear molecular disk. Evidence for such superwinds has been found in Far Infrared Galaxies (FIRGs) (Heckman et al. 1990, H90 hereafter). These galaxies show emission lines with FWHM of several hundreds km s^{-1} and shifted by $\sim$1000 km s^{-1} in some objects. Appropriate superwind models predict outflow velocities of several hundreds km s^{-1}.

We have calculated some basic parameters characterizing a superwind which could explain the kinematic properties of the EELR in HZRG (we want to enphasize the approximate nature of this calculations). We have assumed a typical radius r_{neb} for the ionized nebula of 20 kpc, a density n_0 in the ambient (undisturbed) medium of 10 cm^{-3} (McCarthy 1993). Two emission lines components of several hundred km s^{-1} (unresolved at our spectral resolution) and shifted by 1000 km s^{-1} will produce a broad profile with FWHM$\sim$1000 km s^{-1}, the values observed in our objects. Therefore, we can assume, as concluded for nearby FIRGs, an expanding velocity of the nebula v_{neb} of several hundreds km s^{-1} (500 km s^{-1}). The dynamical time scale t_{dyn} for the nebula is given by Eq. [7] in H90. We obtain t_{dyn} $\sim$40 Myr, which is in the range calculated for some FIRGs. According to the predictions of the superwind models, this is comparable to the age of the starburst. For comparison, Dey et al. (1997) derived an upper limit for the young stellar population in the radio galaxy 4C41.17 (z=3.80) of 600 Myr for a continuous star formation scenario and $\sim$ 16 Myr for an instantaneous starburst model.

On the other hand, if the total mass of the ionized gas (several$\times$10^8-10^9 M$_\odot$, van Ojik 1995, McCarthy 1993) has been ejected in the outflow and t_{dyn} $\sim$40 Myr, this implies that the mass injection rate is 7$\leq \frac{dE}{dt} \leq$25 M$_\odot$ yr^{-1}, which is also consistent with superwind models for nearby FIRGs. We have also calculated the rate of injection of kinetic energy in the wind $\frac{dE}{dt}$, given by Eq. [8] in H90. We obtain $\sim$3$\times$10^{47} erg s^{-1} which is one order of magnitude higher than predicted for high power FIRGs. This is what we expect taking into account cosmological evolution of the wind rate (H90) (the mass injection rate should increase by the same factor, though). $\frac{dE}{dt}$ is large compared to the inte-

grated luminosity of the lines (Lyα can be as luminous as $\sim 10^{44}$ erg s^{-1}).With a small conversion efficiency of kinetic energy of the outflow in emission line luminosity, the outflow could power the nebula.

Therefore, a superwind with properties similar to those predicted for the high power FIRGs at low redshift, could explain the kinematic properties of the extended gas in the HZRG.

The possibility of an outflowing wind generated in the nuclear region of a powerful radio galaxy is suggested by the nearby radio galaxy Cyg A: a polarization map (Tadhunter et al. 1990, Ogle et al. 1997) shows a biconical structure suggestive of a dusty reflection nebula which scatters the light of the hidden active nucleus. The outflow is suggested by the shift between the narrow emission lines detected in direct light and the polarized narrow lines (Ogle et al. 1997). Evidence for a circumnuclear starburst ring is presented in Fosbury et al. 1998a. The velocity shift however, is much lower ($\sim$100–200 km s^{-1}) than the FWHM values observed at high z.

6. Summary and conclusion

We have studied the UV spectra of 3 distant powerful radio galaxies and the hyperluminous SMM J02399-136 system with the goal of understanding the mechanism responsible for the high velocities observed in the extended gas of HZRG. Large velocities are found in the extended gas of all the objects (FWHM$>$1000 km s^{-1}).

Interactions between the radio jet and the ambient gas certainly play a role in some radio galaxies. However, we measure high velocities in regions where such type of interactions are not taking place and therefore other mechanisms must be at work.

Possible explanations for such extreme motions are: 1) infall of material from large distances (gravitational origin). This mechanism could be important in the process of galaxy formation. 2) A group of Ly break galaxies in the neighbourhood of the radio galaxy. Large scale outflows in the individual components are required. 3) Bipolar outflows produced by superwinds, as observed in nearby FIRGs.

Acknowledgements. This work is based on spectroscopic data obtained at La Silla Observatory. M.Villar-Martín acknowledges support of PPARC fellowship to develop most of this work at the Department of Physics and Astronomy in Sheffield (UK). Thanks to the referee, Pat McCarthy, for useful comments that contributed to improve the paper. Thanks also to Raffaella Morganti for helpful comments on the radio and optical astrometry of MRC1558-003.

References

Bremer M., Fabian A., Sargent W., et al., 1992, MNRAS 258, 23
Chambers K.C., Miley G.K., van Breugel W., 1987, Nat 329, 604
Chambers K.C., 1998, in American Astronomical Society Meeting, 193, 110.01
Cimatti A., di Serego Alighieri S., Vernet J., Cohen M., Fosbury R., 1998, ApJ 499, 21
Clark N.E., Tadhunter C.N., Morganti R., et al., 1997, MNRAS 286, 558
Corbin M., Francis P., 1994, AJ 108, 2016
Dey A., van Breugel W., Vacca W., Antonucci R., 1997, ApJ 490, 698
Evans A., 1998, ApJ 498, 553
Fosbury R., Vernet J., Villar-Martín M., et al., 1998a, In: Röttgering, Best, Lehnert (eds.) The most distant radio galaxies. Amsterdam, The Netherlands, October 1997, in press(astro-ph/9803310)
Fosbury R., Vernet J., Villar-Martín M., et al., 1998b, In: Freudling W., Hook R. (eds.) NICMOS and the VLT: A New Era of High Resolution Near Infrared Imaging and Spectroscopy. Pula, Sardinia, Italy, 26–27 June, 1998, ESO Conference and Workshop Proceedings 55, p. 190
Fosbury R., Vernet J., Villar-Martín M., et al., 1999, In: Chemical Evolution from zero to high redshift. Garching, Germany, 14–16 October, 1998, ESO Conference and Workshop Proceedings, submitted
Franx M., Illingworth, Kelson D., van Dokkum P., Tran K., 1997, ApJ 486, L75
Heckman T., Armus L., Miley G., 1990, ApJS 74, 833 (H90)
Heckman T., Lehnert M., Miley G., van Breugel W., 1991, ApJ 381, 373
Ivison R., Smail I., Le Borgne J., et al., 1998, MNRAS 298, 593 (IV98)
Koekemoer A., van Breugel W., Bland-Hawthorn J., 1996, In: Bremer, van der Werf, Röttgering, Carilli (eds.) Cold Gas at High Redshift. Kluwer Academic Publishers, p. 385
Lehnert M., Becker R., 1998, A&A 332, 514
Lowenthal J., 1997, Rev. Mex. Astron. Astrofis. (Serie de Conferencias) 6, 105
McCarthy P.J., Spinrad H., Djorgovsky S., et al., 1987, ApJ 319, L39
McCarthy P.J., Kapahi V., van Breugel W., Subrahmanya C., 1990, AJ 100, 1014
McCarthy P.J., 1993, ARA&A 31, 639
McCarthy P.J., Baum S., Spinrad H., 1996, ApJS 106, 281
Ogle P., Cohen M., Miller J., et al., 1997, ApJL 482, 370
Pentericci L., Röttgering H., Miley G., et al., 1999, A&A 341, 329
Pettini M., Kellog M., Steidel C., et al., 1998, ApJ 508, 539
Prochaska J., Wolfe A., 1997, ApJ 487, 73
Rhee G., Marvel K., Wilson T., et al., 1996, ApJS 107, 175
Röttgering H., Lacy M., Miley G., Chambers K., Saunders R., 1994, A&AS 108, 79
Steidel C., Giavalisco M., Dickinson M., Adelberger K., 1996, AJ 112, 352
Stockton A., Ridgway S., Kellogg M., 1996, AJ 112, 902
Tadhunter C., Fosbury R., Quinn P., 1989, MNRAS 240, 225
Tadhunter C., Scarrot S., Rolph C., 1990, MNRAS 246, 163
van Breugel W., Stanford S., Spinrad H., Stern D., Graham J., 1999, ApJ in press (astro-ph/9803019)
van Ojik R., 1995, Ph.D. Thesis, University of Leiden
van Ojik R., Röttgering H., Carilli C., et al., 1996, A&A 313, 25
Villar-Martín M., Tadhunter C.N., Morganti R., et al., 1998, A&A 332, 479
Villar-Martín M., Tadhunter C.N., Morganti R., Axon D., Koekemoer A., 1999, MNRAS in press